

Atom transfer radical polymerization by $[\text{RuCl}_2(\text{PPh}_3)_2(\text{amine})]$ catalysts: Cyclic amines as tuner of reactivity

Thais R. Cruz¹ · Patrícia Borim^{1,2} · Beatriz E. Goi¹ · José L. Silva Sá³ · Benedito S. Lima-Neto² · Valdemiro P. Carvalho Jr¹

Received: 6 July 2017 / Accepted: 12 October 2017 / Published online: 28 October 2017
© Springer Science+Business Media B.V. 2017

Abstract Atom transfer radical polymerizations (ATRP) of styrene (St) and methyl methacrylate (MMA) mediated by $[\text{RuCl}_2(\text{PPh}_3)_2(\text{amine})]$ complexes, with amine = pyrrolidine (**1**), piperidine (**2**), or perhydroazepine (**3**), were investigated as a function of time, temperature, and concentrations of monomers and 2-bromoisobutyrate as initiator. The plots of $\ln([M]_0/[M])$ vs. time and molecular weights vs. monomer conversion were linear and the dispersity indexes decreased with increasing monomer conversions. The complexes **1**, **2**, and **3** were able to mediate the polymerizations with acceptable rate and level of control. Differences in the rate and control of polymerization were observed in the order $3 > 2 > 1$ for both monomers. The activities were discussed considering the steric hindrance and electronic characteristics of the amines as ancillary ligands in the metal centres, considering studies by cyclic voltammetry and NMR.

Keywords ATRP · Styrene · Methyl methacrylate · Ruthenium · Polymerization

Electronic supplementary material The online version of this article (<https://doi.org/10.1007/s10965-017-1354-9>) contains supplementary material, which is available to authorized users.

✉ Benedito S. Lima-Neto
benedito@iqsc.usp.br

✉ Valdemiro P. Carvalho, Jr
valdemiro@fct.unesp.br

¹ Faculdade de Ciências e Tecnologia, UNESP Univ Estadual Paulista, Presidente Prudente, SP 19060-900, Brazil

² Instituto de Química de São Carlos, Universidade de São Paulo, São Carlos, SP 13560-970, Brazil

³ Centro de Ciências da Natureza, Universidade Estadual do Piauí, Teresina, PI 64002-150, Brazil

Introduction

Transition metal catalyzed controlled/living radical polymerizations of the organometallic-mediated radical and atom-transfer radical (ATRP) types [1–5] are among the most rapid-developing themes in synthetic chemistry, as they provide polymers with predefined functionalities, compositions, and architectures [6–8].

The ATRP mechanism is based on a metal-mediated activation-deactivation equilibrium of propagating radical chains involving the metal species in two oxidation states [7, 9, 10]. The ATRP rate and the control of molecular dispersity depend on the metal redox equilibrium pair. This parameter is strongly influenced by the structure and properties of the starting complex to generate the active metal species, which cannot undergo decomposition when changing the oxidation state. The rational design of each ligand-metal interaction in the starting complex, using established structure-activity relationships, provides a promising strategy to develop superior catalytic systems to improve the ATRP process. Subtle variations in the ligand structure are very important for providing an adjustable redox potential, which reflects in the electronic parameter, and a steric environment in metal complexes. Within this reasoning, ruthenium(II) complexes are promising candidates for the development of active, robust and versatile ATRP catalysts. This is supported by a number of Ru(II)-ligand arrangements from a wide range of designs with electronic and steric parameters, in addition to their high tolerance to the functional group, which allows reactivity in the presence of oxo-organic groups and in polar protic media [11]. This allows tuning of the catalyst for use with a wide array of olefin-based monomers. Ruthenium complexes in low oxidation states, for instance two ($4d^6$) and three ($4d^5$), are low spin and usually used in homogeneous catalysis because the complex lability depends on the thermodynamic influence and kinetic effect of

the coordinated ligands. An example is the $[\text{RuCl}_2(\text{PPh}_3)_3]$ complex, which was investigated by Sawamoto et al. [12, 13] in ATRP of methyl methacrylate with good polymer results. They also investigated how the presence of a Lewis acid can improve reaction control when adjusting Ru(III) reversibility back to Ru(II) species without losing active Ru species by decomposition of the Ru(III)-halide species in solution. A way of controlling the ATRP growing polymer chains is tuning the electronic and steric effects of the ligands on the metal centre, when the $[\text{L}_n\text{Ru(III)-halide}]/\{\text{radical-chain}\}$ couple is shifted back to the $[\text{L}_n\text{Ru(II)}]/\{\text{halide-chain}\}$ couple, taking a ruthenium complex as example. A concern regarding the $[\text{RuCl}_2(\text{PPh}_3)_3]$ complex is the fast discoordination of one PPh_3 molecule due to steric hindrance with incidence of $\{\text{RuCl}_2(\text{PPh}_3)_2\}$ moiety dimerization [14–16], which can interfere in reaction occurrence.

Most of the ruthenium-based ATRP catalyst systems for the polymerization of styrene and various acrylates incorporate phosphines [17–20], a combination of cyclopentadienyl or arene with phosphine ligands [21–24], Fischer or *N*-heterocyclic carbenes [19, 25–30], Schiff base ligands [31–34], bimetallic [35, 36], and amidinate [37]. Few studies have discussed basic amines as additives to improve ATRP [18, 38]. Our research group has successfully developed $\{\text{Ru(II)-PPh}_3\}$ -based complexes of the $[\text{RuCl}_2(\text{PPh}_3)_2(\text{amine})]$ type, with σ -donor cyclic amine ligand in the coordination sphere, which are highly active catalysts for ring-opening metathesis polymerization (ROMP) reactions [39–44]. Recently, the catalytic activity of the $[\text{RuCl}_2(\text{PPh}_3)_2(\text{azocene})]$ complex as a catalyst for ATRP and ROMP reactions was evaluated [45]. On the one hand, the PPh_3 molecule increases the Ru(II) oxidation potential, which prevents reactions with O_2 molecules providing air open handling; on the other hand, the amines supply electrons to forward the reactivity of the active species. Both phosphine and amine adjust the steric hindrance on the coordination sphere, with no large steric hindrance demands. The strategy has proven to be very successful in ROMP with the combination of a strong binding amine ligand and a rather labile phosphine ligand. In ROMP, two free positions in the active species are needed for the reaction can occur. In the case of ATRP, the starting complex can operate without losing a phosphine, where only one open position in the active species is needed. Thus these well-defined amine-based Ru complexes can be applied in ATRP, considering that electronic and steric effects are of fundamental importance for a successful metal-mediate controlled radical reaction. Exploring the Ru(II)/Ru(III) pair in the presence of a coordinated amine as σ -donor ligands to balance the electronic density in the metal centre and the steric hindrance can be a trump card for developing sophisticated new catalysts for ATRP, as well as towards ROMP-ATRP dual process [46].

In this study, we evaluated the application of $[\text{RuCl}_2(\text{PPh}_3)_2(\text{amine})]$ complexes (Fig. 1), with

amine = pyrrolidine (1), piperidine (2), or perhydroazepine (3), as versatile catalyst precursors for ATRP of styrene (St) and methyl methacrylate (MMA) under different conditions of temperature, reaction time, and concentrations of monomers and 2-bromoisobutyrate as initiator. The goal was to observe the ring size influence on catalyst reactivity, discussing the σ -donor nature and steric hindrance of the amines, obtaining resources to understand the factors that influence ATRP efficiency.

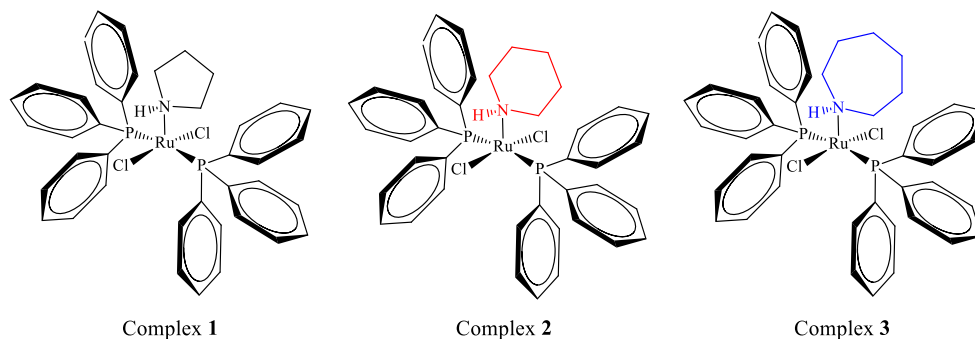
Experimental

General remarks

All reactions and manipulations were performed under an argon atmosphere by using conventional Schlenk-tube techniques. Styrene (St) and methylmethacrylate (MMA) from Aldrich were washed with 5% NaOH solution, dried over anhydrous Mg_2SO_4 , vacuum distilled from CaH_2 and stored at -18°C before use. $\text{RuCl}_3 \cdot x\text{H}_2\text{O}$, anisole, tetrabutylammonium hexafluorophosphate (TBAPF_6), pyrrolidine (pop), piperidine (pip), perhydroazepine (pep) and ethyl 2-bromoisobutyrate (EBiB) from Aldrich were used as acquired. The $[\text{RuCl}_2(\text{PPh}_3)_3]$ complex was prepared following the literature and its purity was checked by satisfactory elemental analysis and spectroscopic examination ($^{31}\text{P}\{^1\text{H}\}$ and ^1H -NMR, FTIR and EPR) [15, 16,].

Analyses

Elemental analyses were performed with a Perkin-Elmer CHN 2400 at the Elemental Analysis Laboratory of Institute of Chemistry - USP. ESR measurements from solid sample were conducted at 77 K using a Bruker ESR 300C apparatus (X-band) equipped with a TE102 cavity and an HP 52152A frequency counter. The FTIR spectra in CsI pellets were obtained on a Bomem FTIR MB 102. Electronic spectra were recorded on a Varian model Cary 500 NIR spectrophotometer, using 1.0 cm path length quartz cells. The ^1H and $^{31}\text{P}\{^1\text{H}\}$ NMR spectra were obtained in CDCl_3 at 298 K on a Bruker DRX-400 spectrometer operating at 400.13 and 161.98 MHz, respectively. The obtained chemical shifts were reported in ppm relative to TMS or 85% H_3PO_4 . Conversion was determined from the concentration of residual monomer measured by gas chromatography (GC) using a Shimadzu GC-2010 gas chromatograph equipped with a flame ionization detector and a 30 m (0.53 mm I.D., 0.5 μm film thickness) SPB-1 Supelco fused silica capillary column. Anisole was added to polymerization and used as an internal standard. Analysis conditions: injector and detector temperature, 250°C ; temperature program, 40°C (4 min), $20^\circ\text{C min}^{-1}$ until 200°C , 200°C (2 min). The molecular weights and the molecular weight

Fig. 1 Illustration of the amineruthenium catalysts **1**, **2** and **3**

distribution of the polymers were determined by gel permeation chromatography using a Shimadzu Prominence LC system equipped with a LC-20 AD pump, a DGU-20A5 degasser, a CBM-20A communication module, a CTO-20A oven at 40 °C and a RID-10A detector equipped with two Shimadzu column (GPC-805: 30 cm, $\varnothing = 8.0$ mm). The retention time was calibrated with standard monodispersed polystyrene using HPLC-grade THF as an eluent at 40 °C with a flow rate of 1.0 mL min⁻¹. Electrochemical measurements were performed using an Autolab PGSTAT204 potentiostat with a stationary platinum disk and a wire as working and auxiliary electrodes, respectively. The reference electrode was Ag/AgCl. The measurements were performed at 25 °C \pm 0.1 in CH₂Cl₂ with 0.1 mol L⁻¹ of *n*-Bu₄NPF₆.

Syntheses of [RuCl₂(PPh₃)₂(amine)] (**1**, **2** and **3**)

The [RuCl₂(PPh₃)₂(amine)] complexes were prepared following the literature [39, 43, 44]. The amine (0.34 mmol) was added to a solution of [RuCl₂(PPh₃)₃] (0.26 mmol; 0.25 g) in acetone (40 mL) and the resulting dark green solution was stirred for 2 h at room temperature. A green precipitate was then filtered and washed with methanol and ethyl ether and then dried in a vacuum.

Complex 1: Yield: 54%; Analytical data for RuCl₂P₂NC₄₀H₃₉ was 62.43 C, 5.18 H and 1.82% N; Calcd. 62.58 C, 5.12 H and 1.82% N. FTIR in CsI: 320 cm⁻¹ [w; ν (Ru–Cl)] was found; 3232 cm⁻¹ [w; ν (pop N-H)]. ³¹P{¹H} NMR (CDCl₃; δ , ppm): 62.6 (s) and 45.3 (s). EPR: no signal was observed.

Complex 2: Yield: 65%; Analytical data for RuCl₂P₂NC₄₁H₄₁ was 63.12 C, 5.35 H and 1.69% N; Calcd. 63.00 C, 5.29 H and 1.79% N. FTIR in CsI: 310 cm⁻¹ [w; ν (Ru–Cl)] was found; 3223 cm⁻¹ [w; ν (pip N-H)]. ³¹P{¹H} NMR (CDCl₃; δ , ppm): 62.7 (s). EPR: no signal was observed.

Complex 3: Yield: 78%; Analytical data for RuCl₂P₂NC₄₂H₄₃ was 63.57 C, 5.73 H and 1.74% N; Calcd. 63.40 C, 5.45 H and 1.76% N. FTIR in CsI: 314 cm⁻¹ [w; ν (Ru–Cl)] was found; 3266 cm⁻¹ [w;

ν (pep N-H)]. ³¹P{¹H} NMR (CDCl₃; δ , ppm): 61.5 (s) and 44.7 (s). EPR: no signal was observed.

Polymerization procedures

In a typical ATRP experiment, 12.3 μ mol of complex was placed in a Schlenk tube containing a magnet bar and capped by a rubber septum. Air was expelled by three vacuum-nitrogen cycles and monomer (St or MMA) and the initiator solution (EBiB) were added. All liquids were handled with dried syringes under nitrogen. The tube was capped under N₂ atmosphere using Schlenk techniques, then the reaction mixture was immediately immersed in an oil bath previously heated to the desired temperature. The samples were removed from the tube after certain time intervals using degassed syringes. The polymerization was stopped when the reaction mixture became very viscous. The reported conversions are average values from catalytic runs performed at least three times.

Results and discussion

Studies for ATRP of St

Catalytic activities of the starting Ru complexes **1**, **2**, and **3** were investigated in the presence of EBiB as initiator. The reactions were performed in toluene as a function of temperature, monomer/EBiB/Ru molar ratio, and reaction time. From each evaluated parameter, the best conditions were selected for further studies. No polymerizations were observed in the absence of these Ru complexes.

The effect of temperature, ranging from 70 to 110 °C, on the Ru catalytic performance with a [St]/[EBiB]/[Ru] = 3000/2/1 M ratio showed gradual increase in monomer conversion with increasing temperature in all cases for 17 h (Fig. 2). The maximum conversion of St was better than 70% at 110 °C, reaching 90% with **3**, whereas less than 20% was obtained at 70 °C. This exemplifies how sensitive the process is to the temperature.

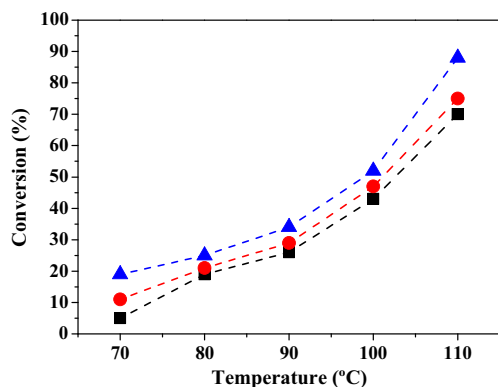


Fig. 2 Dependence of conversion on the reaction temperature for ATRP of St with complexes **1** (■), **2** (●), and **3** (▲); [St]/[EBiB]/[Ru] = 3000/2/1 with 12.3 μmol of Ru in toluene for 17 h

M_n values of the polymers isolated from the experiments under different temperatures show exponential-shaped curves with profile similar to those of the conversion curves (Fig. 3). One order of magnitude higher was obtained, with M_n values increasing from ca. 1×10^4 up to 1×10^5 g mol⁻¹, with decreasing PDI values from ca. 3 units to 1.5. The molecular weights of polySt are not in good agreement with the predicted ones (Fig. 3). Considering that the maximum conversions occurred at 110 °C with polymers with low PDI values, the subsequent studies were performed at this temperature.

Conversion results of the experiments as a function of EBiB amount using a [St]/[Ru] = 3000 ratio for 17 h at 110 °C are shown in Fig. 4. Semi-quantitative conversions with [EBiB]/[Ru] ratio of 3 units were obtained with all the starting complexes, decreasing with increasing [EBiB]/[Ru] ratio. The lowest PDI values were verified with low [EBiB]/[Ru] ratios (Table 1), where the excess of EBiB ([EBiB]/[Ru] > 2) can inhibit the propagation reaction due to termination reactions or transfer chains. The molecular weight decreased with increased [EBiB]/[Ru] ratios. When evaluating

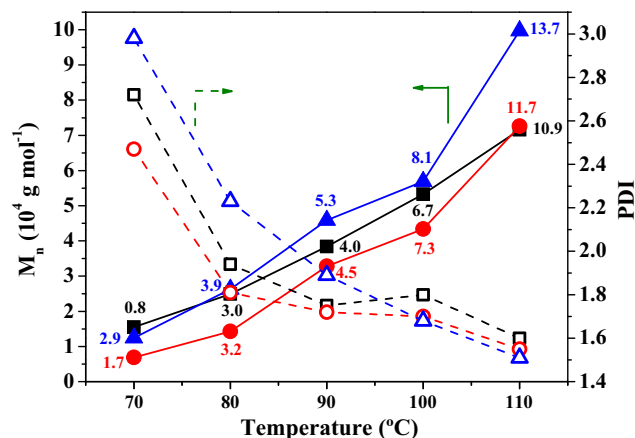


Fig. 3 Dependence of M_n and PDI on the reaction temperature for ATRP of St with complexes **1** (■), **2** (●), and **3** (▲); [St]/[EBiB]/[Ru] = 3000/2/1 with 12.3 μmol of Ru in toluene for 17 h. The inserted numbers are the $M_{n,theor}$ values in 10^4 g mol⁻¹

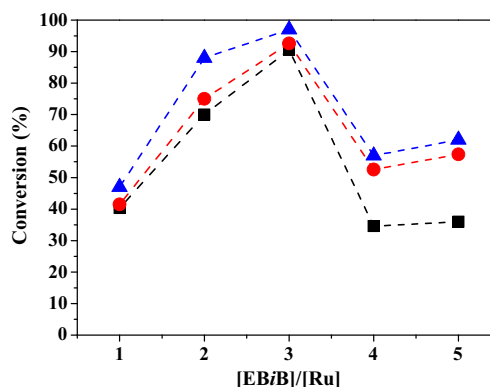


Fig. 4 Dependence of conversion on the [EBiB]/[Ru] ratio for ATRP of St with complexes **1** (■), **2** (●), and **3** (▲); [St]/[Ru] = 3000 with 12.3 μmol of Ru in toluene at 110 °C for 17 h

the relationship between the theoretical and experimental molecular weights of polySt obtained with complexes **1**, **2**, and **3** (initiator efficiency f), the theoretical molecular weights predicted were, in general, higher than those obtained experimentally ($f > 1$) (Table 1), indicating generation of additional polymer chains through transfer reactions. Considering that the lowest values of PDI and initiator efficiency closer to 1 were achieved with [EBiB]/[Ru] = 2, this ratio was selected for the subsequent studies.

Table 1 Results from ATRP of St using complexes **1**, **2**, and **3** in toluene in different amounts of EBiB at 110 °C for 17 h^a

Complex	[EBiB]/[Ru]	Conversion ^b (%)	$M_{n,exp}$ ^c ($\times 10^4$)	$M_{n,theor}$ ^d ($\times 10^4$)	PDI	f
1	1	53	15	8.3	2.03	0.5
	2	70	7.2	11	1.60	1.5
	3	90	3.8	14	1.87	3.7
	4	34	2.6	5.3	1.83	2.0
	5	36	1.6	5.6	2.39	3.5
2	1	41	12	6.4	1.86	0.5
	2	75	7.3	12	1.55	1.6
	3	92	5.7	14	1.79	2.5
	4	52	2.6	8.2	2.00	3.1
	5	57	4.4	8.9	2.29	2.0
3	1	47	13	7.3	1.70	0.6
	2	88	9.9	14	1.51	1.4
	3	97	4.6	15	1.59	3.3
	4	57	4.4	8.9	1.55	2.0
	5	62	3.7	9.6	1.90	2.6

^a [St]/[Ru] = 3000

^b Determined from the concentration of residual monomer measured by gas chromatography

^c Determined with size exclusion chromatography (SEC) with polystyrene calibration

^d $M_{n,theor} = ([St]/[EBiB] \times M_{w,St} \times conversion)/100$

^e efficiency factor $f = M_{n,theor}/M_{n,exp}$

In the experiments conducted as a function of monomer/complex ratio (Fig. 5), the conversion increased up to $[St]/[Ru] = 1500$ following saturation curve profiles with results in the range of 70–95%. The PDI values were roughly the same, regardless of the starting complex type (Fig. 5, insert), and the values tend to increase up to $[St]/[Ru] = 1500$, but they decrease as the amount of monomer increases ($[St]/[Ru] = 3000$).

The molecular weights increased with increasing [monomer]/[Ru] ratio with all the complexes for $[St]/[Ru]$ ratios higher than 500 (Table 2). Although the molecular weights were lower than the calculated values, the PDI values were approximately the same for all of the isolated polymers. There is no clear explanation for the increased M_n value with $[St]/[Ru]$ ratio = 500, whereas the PDI value was similar to those found in the other cases. For high monomer concentration, polymers with higher molecular weights were obtained, and they were closer to their theoretical values.

Studies as a function of time conducted with $[St]/[EBiB]/[Ru] = 3000/2/1$ at 110°C showed increasing conversion from 10 up to 17 h (Fig. 6). The semilogarithmic plots of $\ln([M]_0/[M])$ vs. time were linear, indicating that the radical concentrations are constant throughout the polymerizations. The molecular weights increased linearly with conversion and were close to the calculated ones (Fig. 7). Dispersity indexes are typically ca. 1.5 and decrease with increasing monomer conversion. It is possible to infer that the activity and control level of St polymerization increase in the following order: $1 < 2 < 3$.

Studies for ATRP of MMA

Table 3 summarizes the results from the experiments at different temperatures and with different monomer/initiator/Ru

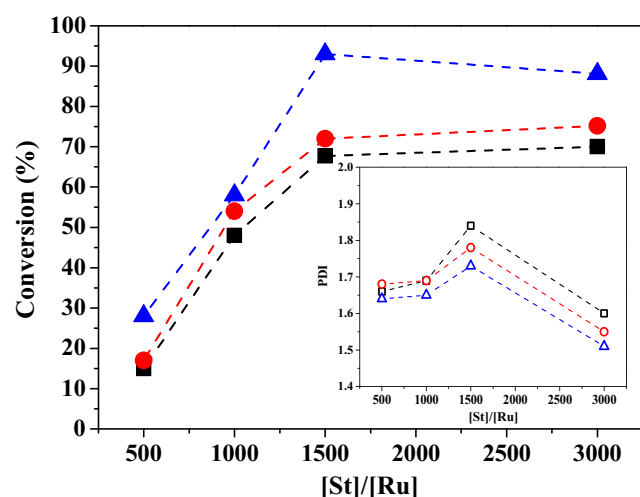


Fig. 5 Dependence of conversion on the $[St]/[Ru]$ ratio for ATRP of St with **1** (■), **2** (●), and **3** (▲); $[EBiB]/[Ru] = 2$ with $12.3 \mu\text{mol}$ of Ru in toluene at 110°C for 17 h. Inset: Dependence of PDI on the $[St]/[Ru]$ ratio for ATRP of St with complexes **1** (■), **2** (●), and **3** (▲)

Table 2 Results from ATRP of St using complexes **1**, **2**, and **3** in toluene in different amounts of St at 110°C for 17 h^a

Complex	$[St]/[Ru]$	Conversion ^b (%)	$M_{n,\text{exp}}$ ^c ($\times 10^4$)	$M_{n,\text{theor}}$ ^d ($\times 10^4$)	PDI	f^e
1	500	15	1.3	0.4	1.7	0.3
	1000	48	0.5	2.5	1.7	5.0
	1500	68	2.2	5.3	1.8	2.4
	3000	70	7.2	11	1.6	1.5
2	500	17	4.6	0.4	1.7	0.1
	1000	54	1.8	2.8	1.7	1.5
	1500	72	1.8	5.6	1.8	3.1
	3000	75	7.2	12	1.5	1.6
3	500	28	12	0.7	1.6	0.06
	1000	58	3.6	3.0	1.6	0.8
	1500	93	6.2	7.2	1.7	1.2
	3000	88	10	14	1.5	1.4

^a $[EBiB]/[Ru] = 2$

^b Determined from the concentration of residual monomer measured by gas chromatography (GC)

^c Determined with size exclusion chromatography (SEC) with polystyrene calibration

^d $M_{n,\text{theor}} = ([St]/[EBiB] \times M_{w,\text{St}} \times \text{conversion})/100$

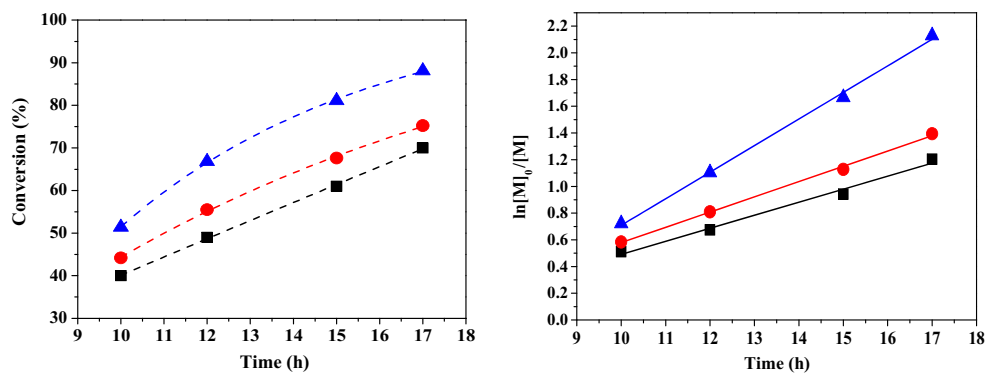
^e efficiency factor $f = M_{n,\text{theor}}/M_{n,\text{exp}}$

ratios, changing the amounts of monomer or initiator. The conversions increased when increasing any of these parameters with any of the complexes, exhibiting the same trend of reactivity observed in the ATRP of St. A significant difference between these results and those obtained for St are the narrower PDI values; most of them were lower than 1.5. The molecular weights were in the same order of magnitude and were similar to the theoretical values, with efficient factor f ranging between 0.5 and 2 units.

Considerations on the reaction mechanism

The increased electron donicity of the ancillary ligands plays an important role in the activity of ATRP catalysts when decreasing the metal redox potential, facilitating halide abstraction from the dormant polymer chains. This would shift the equilibrium towards the growing polymer radicals and, therefore, increase the polymerization rate. The activity of an ATRP catalyst depends mainly on the redox potential of the $M^{n+}/M^{(n+1)+}$ couple and on the halidophilicity of the $M^{(n+1)+}$ complex. The redox potential seems to play a key role for Cu-based catalysts, whereas halidophilicity appears to be more important for Ru-complexes; as for other metal catalysts, the two factors have an intermediate effect [5, 47]. In this context, the redox properties of complexes **1**, **2**, and **3** were measured using cyclic voltammetry techniques to understand their different activities as ATRP catalysts (Fig. S3; Table 4).

Fig. 6 Dependence of conversion (left) and $\ln[M]_0/[M]$ (right) on the reaction time for ATRP of St with complexes **1** (■), **2** (●), and **3** (▲); [St]/[EBiB]/[Ru] = 3000/2/1 with 12.3 μmol of Ru in toluene at 110 °C for 17 h



The small difference in Lewis basicity of the cyclic amine used in the starting complexes with an increase in the CH_2 units in the ring was not sufficient to provide a large change in the anodic potential of the Ru^{II} -amine-based complexes. It was expected that the series of complexes studied exhibits the following order of oxidation behaviour: **1** > **2** > **3**; this provides an indication of activity in ATRP catalysis. This trend cannot be evaluated from the anodic potentials. However, as expected, complexes **1**, **2**, and **3** presented lower anodic potentials than the previously reported precursor $[\text{RuCl}_2(\text{PPh}_3)_3]$ ($E_{\text{ox}} = 0.83$ V vs. Ag/AgCl), and thus were expected to be faster ATRP catalysts [48, 49]. In fact, these complexes have lower redox potentials, but the redox reversibility was not obtained in content. $[\text{RuCl}_2(\text{PPh}_3)_3]$ reversibility was achieved in the presence of $\text{Al}(\text{O}i\text{Pr})_3$, and the authors suggest that an interaction of $\text{Al}(\text{O}i\text{Pr})_3$ with the oxidized metal complex somehow stabilizes the complex in its high oxidation state [48, 49]. However, the electrochemical reversibility of complexes **1**, **2**, and **3** has not been successfully achieved in the presence of Al additive.

Conversion of St and k_{obs} increases as the number of methylene groups in the amine ring (**1** < **2** < **3**) increases, but the

anodic potentials do not follow this order (Table 4). The polymerization rate seems electrochemically illogical because the increase in the oxidation potential for **3**, compared with that of **2**, should disfavour the addition of the halogen atom and, consequently, would retard the polymerization. Therefore, it should be considered that steric factors could

Table 3 ATRP of MMA with complexes **1**, **2**, or **3** under different conditions

Complex	[MMA]/[EBiB]/[Ru]	Temp. (°C)	Conv. ^a (%)	$M_{n,\text{exp}}^b$ ($\times 10^4$)	$M_{n,\text{th}}^c$ ($\times 10^4$)	PDI	f^d
1	3000/2/1	70	28	6.9	4.2	1.32	0.61
	500/2/1	85	26	1.6	0.6	1.74	0.38
	1500/2/1	85	41	5.4	3.1	1.35	0.57
	3000/2/1	85	39	7.1	5.9	1.26	0.83
	3000/2/1	100	54	7.4	8.0	1.49	1.08
	3000/1/1	85	30	13	9.0	1.34	0.67
2	3000/5/1	85	69	2.3	4.1	1.64	1.78
	3000/2/1	70	38	5.0	5.7	1.31	1.14
	500/2/1	85	39	1.1	1.0	1.68	0.91
	1500/2/1	85	45	1.7	3.4	1.48	2.00
	3000/2/1	85	45	6.8	6.7	1.23	0.98
	3000/2/1	100	64	8.8	9.6	1.32	1.09
3	3000/1/1	85	34	13	10	1.27	0.76
	3000/5/1	85	83	2.6	5.0	1.53	1.92
	3000/2/1	70	46	5.4	6.9	1.34	1.27
	500/2/1	85	42	2.6	1.1	1.52	0.42
	1500/2/1	85	60	3.3	4.5	1.34	1.36
	3000/2/1	85	65	9.6	9.7	1.23	1.01
	3000/2/1	100	74	9.7	11	1.35	1.14
	3000/1/1	85	28	9.1	8.4	1.25	0.92
	3000/5/1	85	83	7.3	5.0	1.43	0.68

^a Determined from the concentration of residual monomer measured by gas chromatography

^b Determined with size exclusion chromatography (SEC) with polystyrene calibration

^c $M_{n,\text{theor}} = ([\text{MMA}]/[\text{EBiB}] \times M_{w,\text{MMA}} \times \text{conversion})/100$

^d efficiency factor $f = M_{n,\text{theor}}/M_{n,\text{exp}}$

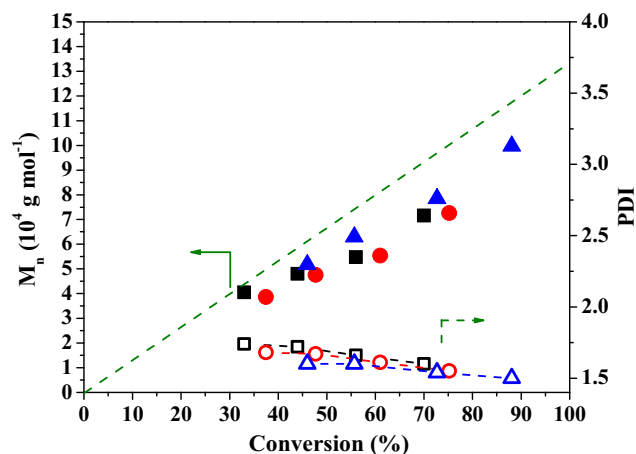


Fig. 7 Dependence of M_n and PDI on the conversion for ATRP of St with complexes **1** (■), **2** (●), and **3** (▲); [EBiB]/[Ru] = 2 and [St]/[Ru] = 3000 with 12.3 μmol of complex in toluene at 110 °C for 17 h; $M_{n(\text{theor})}$ (green dashed line)

Table 4 ATRP of St using complexes **1**, **2**, and **3** in toluene at 110 °C for 17 h for [St]/[EBiB]/[Ru] = 3000/2/1

	E_{anodic} (V; vs. Ag/AgCl)	k_{obs} (10^{-5} s^{-1})	Conv. ^a (%)	$M_{n,\text{exp}}^b$ ($\times 10^4$)	$M_{n,\text{th}}^c$ ($\times 10^4$)	PDI	f^d
1	0.78	2.7	70	7.2	11	1.6	1.5
2	0.73	3.2	75	7.2	12	1.5	1.6
3	0.75	5.5	88	10	14	1.5	1.4

^a Determined from the concentration of residual monomer measured by gas chromatography (GC)

^b Determined with size exclusion chromatography (SEC) with polystyrene calibration

^c $M_{n,\text{theor}} = ([\text{St}]/[\text{EBiB}] \times M_{w,\text{St}} \times \text{conversion})/100$

^d efficiency factor $f = M_{n,\text{theor}}/M_{n,\text{exp}}$

play a decisive role in polymerization rate, where interaction between the metal complex and the initiator or growing polymer radical depends on steric hindrances. The increase in steric hindrance with increasing CH₂ units in the ring should provide greater lability to the halide-complex, shifting the ATRP equilibrium further to the left-hand side, lowering the instantaneous radical concentration, and leading to fewer termination events. In others words, this controls the growing chains.

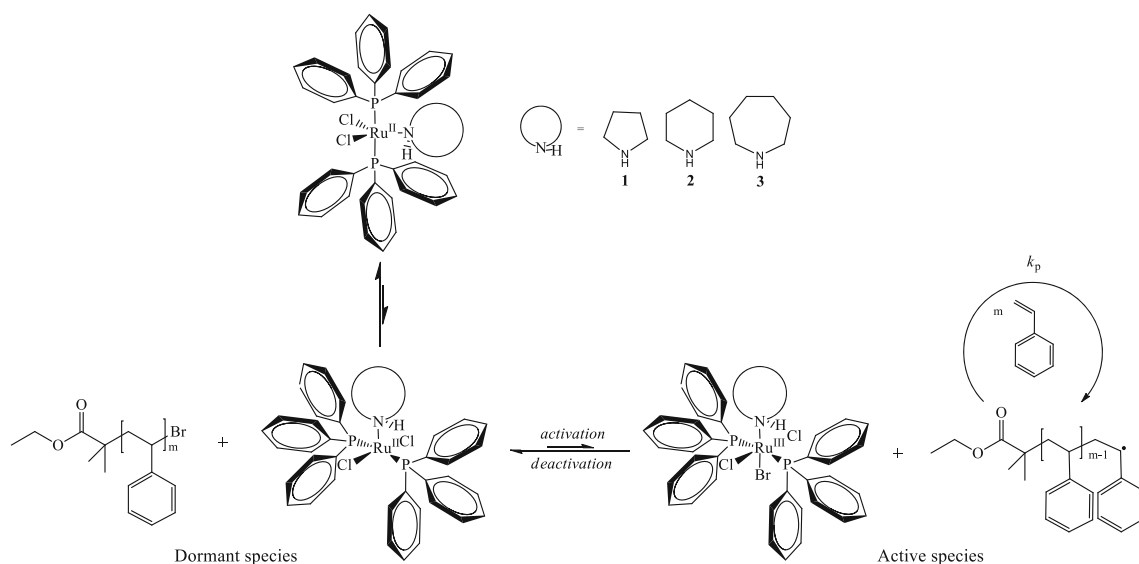
St polymerization catalyzed by complex **3** with the bulkiest ligand was faster than those mediated by complexes **1** and **2** (Table 3), even though the anodic potentials of these catalysts are similar. ATRP with **3** was also better controlled, as it can be estimated from the molecular weight data; the experimental molecular weights were closer to the theoretical values and the narrowest PDI values were also found. Although correlation between reactivity and redox potential can not be established at this point, the steric factor seems to play an essential role in ATRP activity, considering that compounds that feature a

more hindered sixth coordination site show the highest reactivity and better control over the polymerization reaction. Hence, complex **3** showed the best catalytic performance, and its behaviour could not be accounted for just in terms of electrochemical properties.

ATRP reactions mediated by complexes **1**, **2**, or **3** were investigated by ³¹P{¹H} NMR. The NMR spectra showed signals associated with the starting species in solution at room temperature. Two sharp signals at 62.7 and 45 ppm in the spectra suggest the presence of isomer complexes with square pyramidal (SQP) and trigonal bipyramid (TBP) type geometries (Scheme 1), respectively [39, 43, 44]. The spectra of the solutions in the presence of EBiB and St showed that the SQP-geometry species is completely consumed after 30 min of reaction at 85 °C, confirming that this species is responsible for activating the ATRP reaction. The TBP-geometry species is only slowly consumed during polymerization. Perhaps, the TBP-geometry species changes to the SQP-geometry type to become active for ATRP.

Conclusion

Catalytic activities of the amine-Ru complexes **1**, **2**, and **3** were successfully investigated in the ATRP of St or MMA. The temperature, reaction time, and amounts of monomer and initiator enhanced the conversions, with polymerization control somewhat tuned by the type of amine ligand. Molecular weights increased with conversion and were not very discordant from the calculated ones. The PDI values decreased with increasing monomer conversion in all cases. The polymerization rate and control level increased in the following order: **1** < **2** < **3**. It was established that the number of CH₂ units in the amine ring can be responsible for the catalytic behaviour.

**Scheme 1** Possible reaction routes for ATRP of St mediated by complexes **1**, **2**, or **3**. The termination step was omitted for simplification and clarity

Comparison between the reactivity of complexes **1**, **2**, and **3** and the electrochemical data suggests that the efficiency of using these types of complexes seems to be induced by steric factors; however, electronic effects should also be considered. Furthermore, from studies with $[\text{RuCl}_2(\text{PPh}_3)_3]$ and other Ru complexes, the activities of the amine-Ru complexes **1**, **2**, and **3** were higher [19, 22, 26, 35, 49–53], and this fact can be associated with the amines as ancillary ligands, which are not dis-coordinated over the reaction.

Acknowledgements The authors are indebted to the financial support from FAPESP (Proc. 2013/10002-0).

References

1. Poli R (2006). *Angew Chem* 45:5058–5070
2. Poli R (2011). *Eur J Inorg Chem* 10:1513–1530
3. Kamigaito M, Ando T, Sawamoto M (2001). *Chem Rev* 101:3689–3746
4. Matyjaszewski K, Xia JH (2001). *Chem Rev* 101:2921–2990
5. di Lena F, Matyjaszewski K (2010). *Prog Polym Sci* 35:959–1021
6. Tsarevsky NV, Matyjaszewski K (2007). *Chem Rev* 107:2270–2299
7. Matyjaszewski K (2012). *Macromolecules* 45:4015–4039
8. Matyjaszewski K, Tsarevsky N-V (2009). *Nat Chem* 1:276–288
9. Tang W, Matyjaszewski K (2006). *Macromolecules* 39:4953–4959
10. Tang W, Kwak Y, Braunecker W, Tsarevsky N-V, Coope M-L, Matyjaszewski K (2008). *J Am Chem Soc* 130:10702–10713
11. Naota T, Takaya H, Murahashi S (1998). *Chem Rev* 98:2599–2660
12. Ando T, Kamigaito M, Sawamoto M (1997). *Tetrahedron* 53:15445–15457
13. Ueda J, Matsuyama M, Kamigaito M, Sawamoto M (1998). *Macromolecules* 31:557–562
14. Armit P-W, Boyd A-F, Stephenson T A (1975) *J Chem Soc Dalton Trans* 22:1663–1672
15. Hoffman P-R, Caulton K-G (1975). *J Am Chem Soc* 97:4221–4228
16. Vriends R-J, Kotten G-V, Vrieze K (1978). *Inorg Chim Acta* 26:L29–L31
17. Takahashi H, Ando T, Kamigaito M, Sawamoto M (1999). *Macromolecules* 32:6461–6465
18. Hamasaki S, Kamigaito M, Sawamoto M (2002). *Macromolecules* 35:2934–2940
19. Simal F, Demonceau A, Noels A-F (1999). *Angew Chem Int Ed* 38:538–540
20. Quebatte L, Haas M, Solari E, Scopelliti R, Nguyen Q-T, Severin K (2005). *Angew Chem Int Ed* 44:1084–1088
21. Watanabe Y, Ando T, Kamigaito M, Sawamoto M (2001). *Macromolecules* 34:4370–4374
22. Kamigaito M, Watanabe Y, Ando T, Sawamoto M (2002). *J Am Chem Soc* 124:9994–9995
23. Tutusaus O, Delfosse S, Simal F, Demonceau A, Noels A-F, Núñez R, Viñas C, Teixidor F (2002). *Inorg Chem Commun* 5:941–945
24. Braunecker W-A, Brown W-C, Morelli B-C, Tang W, Poli R, Matyjaszewski K (2007). *Macromolecules* 40:8576–8585
25. Simal F, Sebille S, Hallet L, Demonceau A, Noels A-F (2000). *Macromol Symp* 161:73–85
26. Simal F, Jan D, Delaude L, Demonceau A, Spirlet M-R, Noels A-F (2001). *Can J Chem* 79:529–535
27. Simal F, Delfosse S, Demonceau A, Noels A-F, Denk K, Kohl F, Weskamp J-T, Herrmann W-A (2002). *Chem Eur J* 8:3047–3052
28. Bielawski CW, Louie J, Grubbs RH (2000). *J Am Chem Soc* 122:12872–12873
29. Delaude L, Delfosse S, Richel A, Demonceau A, Noels A-F (2003) *Chem Commun* 0:1526–1527
30. Richel A, Delfosse S, Cremasco C, Delaude L, Demonceau A, Noels A-F (2003). *Tetrahedron Lett* 44:6011–6015
31. De Clercq B, Verpoort F (2002). *J Mol Catal A Chem* 180:67–76
32. De Clercq B, Verpoort F (2002). *Macromolecules* 35:8943–8947
33. Opstal T, Verpoort F (2003). *Angew Chem Int Ed* 42:2876–2879
34. De Clercq B, Verpoort F (2003). *Polym Bull* 50:153–160
35. Sauvage X, Borguet Y, Noels A-F, Delaude L, Demonceau A (2007). *Adv Synth Catal* 349:255–265
36. Haas M, Solari E, Nguyen Q-T, Gautier S, Scopelliti R, Severin K (2006). *Adv Synth Catal* 348:439–442
37. Motoyama Y, Hanada S, Niibayashi S, Shimamoto K, Takaoka N, Nagashima H (2005). *Tetrahedron* 61:10216–10226
38. Melis K, Verpoort F (2003). *J Mol Catal A Chem* 201:33–41
39. Matos J-E, Lima-Neto B-S (2004). *J Mol Catal A Chem* 222:81–85
40. Matos J-E, Lima-Neto B-S (2006). *J Mol Catal A Chem* 259:286–291
41. Silva Sá J-L, Lima-Neto B-S (2009). *J Mol Catal A Chem* 304:187–190
42. Carvalho V-P, Ferraz C-P, Lima-Neto B-S (2010). *J Mol Catal A Chem* 333:46–53
43. Silva Sá J-L, Vieira L-H, Nascimento E-P, Lima-Neto B-S (2010). *Appl Catal A* 374:194–200
44. Fonseca L-R, Silva Sá J-L, Nascimento E-P, Lima-Neto B-S (2015). *New J Chem* 39:4063–4069
45. Silva R-N, Borim P, Fonseca L-R, et al. (2017). *Catal Lett* 147:1144–1152
46. Dragutan V, Dragutan I (2006). *J Organomet Chem* 691:5129–5147
47. Braunecker WA, Tsarevsky NV, Gennaro A, Matyjaszewski K (2009). *Macromolecules* 42:6348–6360
48. Ando T, Kamigaito M, Sawamoto M (2000). *Macromolecules* 33:6732–6737
49. Camerano J-A, Rodrigues A-S, Rominger F, Wadepohl H, Gade L-H (2011). *J Organomet Chem* 696:1425–1431
50. Opstal T, Verpoort F (2003). *Polym Bull* 50:17–23
51. Villa-Hernández A-M, Rosales-Velázquez C-P, Saldívar-Guerrab E, Torres-Lubián J-R (2011). *J Braz Chem Soc* 22:2070–2077
52. Aguilar-lugo C, Le Lagadec R, Ryabov A-D, Valverde G-C, Morales S-L, Alexandrova L (2009). *J Polym Sci Part A Polym Chem* 47:3814–3828
53. Opstal T, Verpoort F (2003). *New J Chem* 27:257–262